DOI 10.1007/s11182-019-01866-x

Russian Physics Journal, Vol. 62, No. 8, December, 2019 (Russian Original No. 8, August, 2019)

THE INFLUENCE OF THERMOMECHANICAL TREATMENT CONDITIONS ON CHARACTERISTICS OF STRUCTURAL-PHASE TRANSFORMATIONS AND LEVEL OF MECHANICAL PROPERTIES OF VANADIUM ALLOYS OF DIFFERENT SYSTEMS

K. V. Grinyaev,[1,2] I. A. Ditenberg,[1,2] A. N. Tyumentsev,[1,2] I. V. Smirnov,[1,2] and V. M. Chernov[3]

UDC 548.4; 669:621.039; 669-17; 620.186.8

The data on the influence of thermomechanical treatment modes on characteristics of the short-term strength and plasticity of vanadium alloys of different systems (V–Ti–Cr, V–Zr–C, V–Cr–Zr, V–Cr–W–Zr, V–Cr–Ta–Zr) *are generalized. It is shown that an application of a modified mode ensures an appreciable increase in the short-term strength at room temperature and elevated temperatures, while maintaining an acceptable plasticity. The principal mechanisms of metastable carbide transformations into oxicarbonitride phase particles with phase-forming elements participation and the conditions of their realization are discussed.*

Keywords: vanadium alloys, thermomechanical treatment, microstructure, mechanical properties.

INTRODUCTION

According to [1–3], one of the main requirements to low-activation vanadium alloys used in the new-generation atomic and nuclear fusion reactors is their high-temperature strength at an acceptable level of plasticity. It was shown in a number of studies [4–6] that the vanadium alloys after their manufacturing are frequently characterized by the presence of segregational heterogeneities and second-phase coarse particles, which reduces their service properties. This problem is being solved by developing new methods for grain- and heterophase structure modification. For instance, the methods of thermomechanical treatments (TMT) are often applied [4–13], which consist in the use of a number of deformation and heat-impact cycles.

In the present work we provide a generalization of the experimental data on the influence of the standard and modified TMT-modes on the characteristics of short-term strength and plasticity of low-activation vanadium alloys of different systems.

EXPERIMENTAL MATERIALS AND PROCEDURES

Table 1 lists the alloy compositions used in this study, which were produced at SC VNIINM (Moscow, Russia).

The alloys were subjected to heat treatments in vacuum at $\approx 2 \cdot 10^{-5}$ Torr. The cooling rate after annealing within the temperature range of the secondary-phase precipitation varies during cooling from about 5 deg/s (at $T \approx 1200$–1300°C) to 1 deg/s (at $T \leq 800$°C).

[1]Institute of Strength Physics and Materials Science of the Siberian Branch of the Russian Academy of Sciences, Tomsk, Russia, e-mail: kvgrinyaev@inbox.ru; ditenberg_i@mail.ru; smirnov_iv@bk.ru; [2]National Research Tomsk State University, Tomsk, Russia, e-mail: tyuments@phys.tsu.ru; [3]SC Bochvar High-Technology Scientific Research Institute for Inorganic Materials, Moscow, Russia, e-mail: chernovv@bochvar.ru. Translated from Izvestiya Vysshikh Uchebnykh Zavedenii, Fizika, No. 8, pp. 159–165, August, 2019. Original article submitted June 25, 2019.

TABLE 1. Vanadium Alloy Compositions

Alloy […]	Content of alloying elements, wt. % (at. %)							
	Cr	Zr	Ti	W	Ta	O	N	C
V–Ti–Cr [4, 6, 7]	4.36 (4.26)	–	4.21 (4.47)	–	–	0.02 (0.06)	0.01 (0.04)	0.01 (0.05)
V–Zr–C [11]	–	2.40 (1.34)	–	–	–	0.04 (0.13)	0.01 (0.04)	0.25 (1.06)
V–Cr–Zr [12]	8.75 (8.62)	1.17 (0.66)	–	0.14 (0.04)	–	0.02 (0.06)	0.01 (0.04)	0.01 (0.04)
V–Cr–W–Zr [12]	4.23 (4.41)	1.69 (1.00)	–	7.56 (2.23)	–	0.02 (0.07)	0.01 (0.04)	0.02 (0.09)
V–Cr–Ta–Zr [13]	6.80 (6.99)	0.79 (0.46)	–	–	6.10 (1.80)	0.05 (0.17)	0.01 (0.03)	0.03 (0.14)

The initial specimens of these alloys represented 1- and 3-mm thick sheets manufactured by a traditional TMT (TMT I in what follows), whose main stages are described below [4, 6, 7, 11–13]:

1. Eight-hour homogenizing annealing of the ingot at the temperature 1300°C.
2. Extrusion (pressing) at elevated temperature.
3. Several cycles of rolling and upsetting at room temperature with intermediate vacuum anneals at the temperature T = 950–1000°C.
4. Stabilizing one-hour annealing at the temperatures 1000 and 1100°C.

An application of TMT II ensures nanostructuring of the heterophase structure via implementation of the mechanism of phase transformations by dissolution of metastable vanadium carbides followed by precipitation of a stable phase from the solid solution [4, 6, 7, 11–13]. This treatment was performed after the 3-rd stage of TMT I and included four-hour vacuum annealing of the specimens at T = 1400°C (1800°C for the V–Zr–C system) and a few (not fewer than 3) TMT-cycles: rolling to ε = 30–50% at room temperature + annealing at T = 600–700°C. For the resulting structure to stabilize, one-hour annealing was performed at 1000 or 1100°C.

The structural investigations were carried out by the methods of transmission electron microscopy using Philips CM 30 TWIN and Philips CM 12 electron microscopes at the accelerating voltages 300 and 120 kV, respectively. Thin foils for the analysis were manufactured by jet electropolishing in a MIKRON-3 facility in a 20%-solution of sulfuric acid in methanol at a voltage of 15 V.

The metallographic examinations were performed in the Olympus GX-71 and NEOPHOT-21 optical microscopes. The metallographic sections were prepared in the section perpendicular to the rolling plane by mechanical grinding followed by electropolishing using the above-described regime.

The mechanical tests of the specimens were carried out by the method of active tension in vacuum (~$2\cdot10^{-5}$ Torr) at a strain rate of $\dot{\varepsilon} \approx 2\cdot10^{-3}$ s^{-1}.

RESULTS AND DISCUSSION

Table 2 presents the averaged values of the short-term strength ($\sigma_{0.1}$) and plasticity (δ) of vanadium alloys of different systems at room temperature versus the treatment and stabilizing annealing temperature.

An analysis of the data listed in Table 2 demonstrates that the use of TMT II ensures an increase in the short-term strength values $\sigma_{0.1}$ at room temperature in the range from about 7 to 44%, depending on the elemental composition of the alloys. Note that the plasticity of the experimental alloys either retains at the same level, or slightly increases. In the case of stabilizing annealing at 1000°C (Table 2), the lowest short-term strengths in the absolute values are demonstrated by the V–Ti–Cr alloy (No. 1, Table 2) after TMT II. An increase in the stabilizing annealing temperature to 1100°C (Nos. 3–5, Table 2) gives rise to a decrease in $\sigma_{0.1}$ of the V–Cr–Zr and V–Cr–W–Zr alloys by

TABLE 2. Averaged Values of Short-Term Strength ($\sigma_{0.1}$) and Plasticity (δ) of Vanadium Alloys of Different Systems at Room Temperature

No.	Alloy […]	TMO I (T = 1000°C)		TMO II (T = 1000°C)		TMO I (T = 1100°C)		TMO II (T = 1100°C)	
		$\sigma_{0.1}$, MPa	δ, %	$\sigma_{0.1}$, MPa	δ, %	$\sigma_{0.1}$, MPa	δ, %	$\sigma_{0.1}$, MPa	δ, %
1	V–Ti–Cr [4, 6, 7]	300	20	327	17	–	–	–	–
2	V–Zr–C [11]	290	20	385	15	–	–	–	–
3	V–Cr–Zr [12]	240	25	345	20	280	25	302	23
4	V–Cr–W–Zr [12]	300	25	380	23	320	22	338	25
5	V–Cr–Ta–Zr [13]	–	–	–	–	263	24	310	28

TABLE 3. Averaged Values of Short-Term Strength ($\sigma_{0.1}$) and Plasticity (δ) of Vanadium Alloys of Different Systems at Elevated Test Temperatures

No.	Alloy […]	T_t, °C	TMO I (T = 1000°C)		TMO II (T = 1000°C)		TMO I (T = 1100°C)		TMO II (T = 1100°C)	
			$\sigma_{0.1}$, MPa	δ, %	$\sigma_{0.1}$, MPa	δ, %	$\sigma_{0.1}$, MPa	δ, %	$\sigma_{0.1}$, MPa	δ, %
1	V–Ti–Cr [4, 6, 7]	800	180	18	235	11	–	–	–	–
2	V–Zr–C [11]	800	180	15	270	16	–	–	–	–
3	V–Cr–Zr [12]	800	180	26	245	8	184	22	210	15
		900	–	–	173	23	–	–	–	–
4	V–Cr–W–Zr [12]	800	190	25	265	12	195	20	205	23
		900	–	–	190	30	–	–	–	–
5	V–Cr–Ta–Zr [13]	800	–	–	–	–	160	26	175	26

more than 10%, but the absolute values are commensurable with those of the V–Ti–Cr alloy after TMT II, annealed at 1000°C.

The mechanical properties at elevated test temperatures (T_t = 800 and 900°C) are given in Table 3. One can see that the modification of structural-phase state using TMT II provides a higher level of strength properties (Table 3) compared to that after TMT I at an acceptable plasticity.

The alloys of the V–Ti–Cr system (No. 1, Table 3) after TMT II accompanied by stabilizing annealing at 1000°C are characterized by the minimal values of $\sigma_{0.1}$ under tensile loading at 800°C. On the other hand, the V–Cr–Zr and V–Cr–W–Zr alloys (Nos. 3, 4, Table 3) not only exhibit higher strength properties at 800°C, but also under tension at 900°C the level of properties is not lower than that in the V–Ti–Cr alloy after TMT I followed by final annealing at 1000°C. Moreover, when the stabilizing annealing temperature is increased to 1100°C, the short-term strength at 800°C still remains at a high level.

The investigations performed [4, 6, 7, 11–13] demonstrated that the efficiency of modifying the grain and heterophase structure during TMT is determined by the conditions necessary for the transformation of the initial coarse second-phase particles precipitated during cooling of the ingot after its melting. It is critical to note that the vanadium alloys presented in Tables 1–3 differ not only in the elemental compositions of their matrices, but also in the interstitial impurity concentrations, which predetermines the phase composition of the interstitial phase particles.

After TMT I, the presence of stitch-like precipitates and segregational heterogeneities (Fig. 1*a*), whose propagation direction is nearly parallel to the rolling direction (RD). The defect, grain, and heterophase structures are characterized by high heterogeneity [4, 6, 7, 11–13]. The second-phase precipitates represent oxycarbonitride particles of different shapes, dispersion, and composition: coarse-dispersed lamellar precipitates (up to 20 μm in length and up to 0.5 μm in thickness) in stitch-like configurations, and coarse equiaxed particles (measuring up to 1–2 μm), which precipitate during cooling of the ingot after its melting. A partial dispersion of the above-mentioned coarse-dispersed precipitates during TMT I results in the formation of particles measuring from tens of nanometers to tenths of

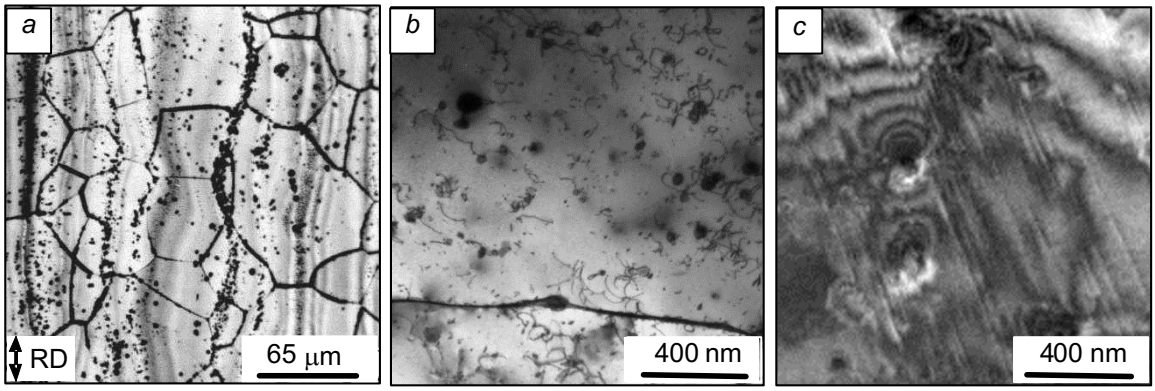

Fig. 1. Microstructure of vanadium alloys after TMT I followed by final annealing at 1000°C: *a* – metallographic images (V–Ti–Cr alloy [8]), *b* – particles in V–Ti–Cr alloy [4, 7], *c* –traces of plastic relaxation of local stresses in V–Cr–W–Zr alloy [12], *b*, *c* – TEM-images.

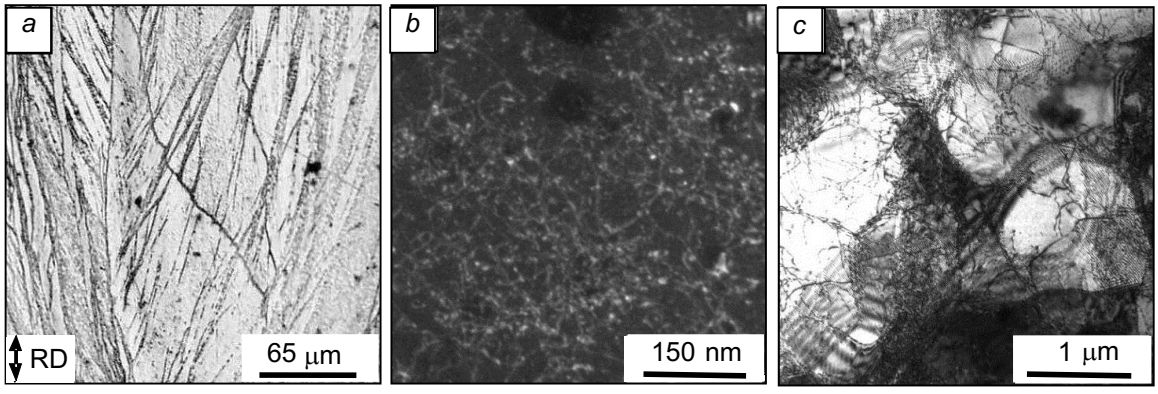

Fig. 2. Microstructure of the alloys after TMT II and final annealing at 1000°C: *a* –V–Ti–Cr alloy microstructure (optical metallography), *b* – fine disperse particles of interstitial phases in V–Cr–Zr–W alloy, *c*– polygonal structure of V–Ti–Cr alloy [7], *b*, *c* – TEM-image.

a nanometer (Fig. 3*b*). The distribution of submicron particles is predominantly homogeneous, while that of nanosized particles is typically inhomogeneous. Furthermore, submicron particles are the sources of high local stresses in the bulk of the grains and at their boundaries. The traces of plastic relaxation of these stresses in the form of slip steps observed in the vicinity of grain boundaries (Fig. 3*c*) imply that they exceed the yield strength value.

It was reported in [4, 6, 7, 11–13] that the heterophase state inhomogeneity after TMT I results in the grain-structure inhomogeneity of the alloys followed by the formation of the regions of primary recrystallization with an elevated density of dislocations pinned by the particles, collective recrystallization zones, and polygonal structure elements.

The use of TMT II favors removing the stitch precipitates and segregation interlayers (Fig. 2*a*), which promotes the formation of a more homogeneous structural state. Furthermore, there is a development of high density of fine-disperse particles (Fig. 2*b*), fostering the stabilization of polygonal and dislocational substructure (Fig. 2*c*) [4, 6, 7, 11–13].

It was shown in [7, 11–13] that the second phases in the analyzed alloys primarily represent FCC-lattice compounds. The calculation of the cumulative volume fraction (*f*) of the second phases (Table 4) in these alloys was performed using the data on their chemical compositions (Table 1). The main phase-forming elements in forming the

TABLE 4. Theoretical Estimates of Cumulative Fraction f of Second Phases

Alloy	V–Ti–Cr	V–Zr–C	V–Cr–Zr	V–Cr–W–Zr	V–Cr–Ta–Zr
f	0.0024	0.0200	0.0016	0.0025	0.0047

TABLE 5. Orowan Stress Estimates in Vanadium Alloys versus Volume Fractions of Fine-Disperse Particles and their Dimensions

Volume fraction of second phase in the form of fine-disperse particles, f_{disp}	Particle size (diameter – 2R), nm		
	5	10	20
	Orowan stress Δσ, MPa		
0.0024	527	264	132
0.0018	457	228	114
0.0012	373	186	93
0.0006	264	132	66
0.00015	132	66	33

carbide (ZrC), oxide (ZrO_2) and complex oxycarbonitrides ($TiV_x(C, O, N)_{1-x}$) compounds were Ti and Zr. It was also assumed that V forms a continuous series of solid solutions with Cr, W and Ta.

In order to determine the dispersion hardening efficiency, we estimated the Orowan stress values as a function of the heterophase structure parameters using the formula [14]

$$\Delta\sigma = Gb/\lambda, \quad (1)$$

where $G \approx 47000$ MPa [15] is the shear modulus of vanadium, $b \approx 0.262$ nm is the Burgers dislocation vector, $\lambda \approx R(2\pi/3f_{disp})^{1/2}$ is the spacing between the particles, R is the particle radius, f_{disp} is the volume fraction of particles in the disperse state. The Orowan stress estimates are listed in Table 5.

It is clear from the estimates (Table 5) that high values of Δσ (from 30 to 110 MPa, Tables 2 and 3) can be achieved at a relatively small volume fraction of the second phase in the form of fine-disperse particles (f_{disp}). TMT II of vanadium alloys (V–Ti–Cr [4, 6, 7], V–Cr–W–Zr [12], V–Cr– Ta–Zr [13], V–Zr–C [11]) ensures an effective transformation of coarse-disperse precipitates into nanoparticles measuring from 5 to 20 nm. The alloys considered in this study essentially differ in their second-phase content (f) from 0.0016 (≈0.16%) in the case of V–Cr–Zr to 0.02 (≈2%) in the V–Zr–C alloy (Table 4). Table 5 suggests that the discussed yield strength increment can be achieved by transforming a minor part of the initial coarse-disperse precipitates into a nanophase state. A considerable increase in Δσ, from our perspective, occurs due to the refinement of the particle size during the stabilization annealing temperature decrease and the high efficiency of strengthening by non-metallic phase particles in the process of overcoming them by sliding dislocations by the Orowan-type mechanism – bending with the elements of fast dislocation climb [16]. A uniform volumetric distribution of fine-disperse particles of minimal sizes ensures the maximum efficiency of disperse-particle strengthening. Unfortunately, it is practically impossible to estimate the contributions from the particle size fractions.

The key features in modification of the heterophase structure of vanadium alloys by the TMT modes I and II are associated with the formation of kinetic conditions determining the mechanism of phase transformations [4, 6, 7, 11–13, 17]. In the carbide-hardened vanadium alloys, the transformation of metastable carbides into the particles of stable oxycarbonitride phases, involving a phase-forming element, can occur via two major mechanisms [5, 7]. The first mechanism, an ‘on site’ transformation (Fig. 3*a*, *b*; I: $b \rightarrow a$), is implemented in when the reaction of stable phase formation occurs in the regions where the metastable phases are found. The second mechanism is realized through dissolution of metastable vanadium carbides followed by precipitation of stable phases from the solid solution (Fig. 3*b*, *c*; II: $b \rightarrow c$).

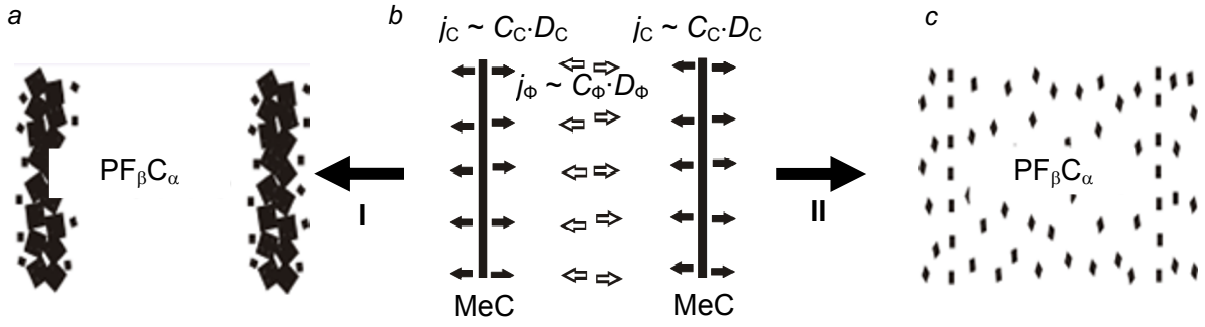

Fig. 3. Transformation of metastable vanadium carbides via an 'on site' transformation (I: $b \rightarrow a$) and by dissolution followed by precipitation of a stable phase from the solid solution (II: $b \rightarrow c$).

In accordance with [4, 7, 17], the mechanisms of metastable-phase transformation during TMT depend on the kinetic parameter

$$K = \frac{C_C \cdot D_C}{C_{PF} \cdot D_{PF}}, \tag{2}$$

where C_C is the carbon concentration, C_{PF} is the concentration of an active phase-forming (PF) element (titanium zirconium, etc.), D_C and D_{PF} are the diffusion coefficients of these elements, respectively. The numerator in the above ratio characterizes the degree of specimen saturation with carbon, and the denominator – the rate of particle formation.

It was shown in [4, 18–20] that during TMT of BCC-alloys the kinetic parameter is mostly affected by the degree of plastic strain, due to increased diffusion flows of phase-forming elements in the fields of high local internal-stress gradients, and the temperature, due to different temperature dependences of the diffusion coefficients of interstitial impurity and phase-forming element.

According to [17], the mechanism of an 'on site' transformation of metastable particles (Fig. 3, I: $b \rightarrow a$) in the heterophase BCC-alloys is realized under the following condition:

$$K << \left(\frac{\alpha}{\beta}\right) C_{PF} \left(\frac{\Delta h}{2 \cdot R}\right)^2, \tag{3}$$

where α, β are the stoichiometric coefficients of the ($PF_\beta C_\alpha$)-phase, Δh is the spacing between the metastable second-phase (MeC) particles, R is the radius of the particles precipitated from the solid solution.

A considerable decrease in the kinetic parameter could be achieved at the treatment temperatures $\geq 0.6 T_{melt}$, for which the diffusion coefficients of phase-forming elements are much (10^4–10^5) higher than those of the interstitial impurities [21]. Therefore, the 'on site' transformation occurs at a high diffusion mobility of phase-forming elements [4, 17], during which the phase-forming elements (such as Ti or Zr) substitute the matrix (alloy) atoms in the metastable phase without dissolution of the latter or its partial solution (Fig. 3*a*, *b*).

At 1000°C (in the case of TMT I), the distance between the coarse-disperse metastable particles in the vanadium alloys in question is about $\Delta h \approx 10$ μm, and the respective estimates of the kinetic parameter ($K \approx 10$–80) indicate a fulfillment of the condition of realization of the 'on site' transformation mechanism.

It was demonstrated [4, 6, 7], using alloys of the V–Ti–Cr system as an example, that an 'on site' transformation of the VC→Ti(V)C-type is possible at a relatively high diffusion-induced mobility of the alloying carbide-forming elements under the conditions of TMT I. In this case, the active carbide-forming element (Ti) substitutes for vanadium atoms without dissolving this phase or with its partial solution. If the rate of solution of metastable-phase precipitates exceeds the rate of supply of titanium atoms into the reaction zone, stable carbide

particles are formed from the solid solution in the vicinity of the metastable precipitates. The second-phase distribution character after the VC→Ti(V)C-transformation is therefore determined by the dispersion and character of the metastable-phase distribution, on the one hand, and by the parameters (diffusion coefficients and diffusion-element content in the solid solution) controlling the titanium and carbon flow intensity in the reaction zone, on the other hand. Similar processes of heterophase structure transformation under TMT I are also observed in vanadium alloys of other systems, where Zr is the phase-forming element.

It has been shown that the particles being formed are of submicron and micron dimensions, and they are sources of high local stresses in the bulk of the grains and at their boundaries (Fig. 1*c*) [4], and in the case of stitch precipitates (along the rolling direction) they can initiate cracking.

The principles of the second transformation mechanism are similar to those taking place in the processes of non-equilibrium internal oxidation [17]. A phase transformation of the VC→TiVC or VC→ZrC type in vanadium alloys (V–Ti–Cr, V–Zr–C, V–Cr–Zr, V–Cr–W–Zr, V–Cr–Ta–Zr) could be treated as carbidizing from internal sources – particles of metastable oxycarbonitrides.

For the mechanism of stable-phase formation to be realized during treatment (TMT II) via dissolution of metastable particles followed by their precipitation from the solid solution (Fig. 3, I: $b \rightarrow c$), according to [17] the following condition has to be fulfilled:

$$K \geq \left(\frac{\alpha}{\beta}\right) C_{\mathrm{PF}} \left(\frac{\Delta h}{2 \cdot R}\right)^2 . \qquad (4)$$

An implementation of this mechanism is determined by the fact that in the case where condition (4) takes place, the rate of the metastable phase solution would exceed the rate of supply of the phase-forming element into the reaction zone [4, 17].

In the vanadium alloys analyzed in this study, the mechanism of formation of fine-disperse particles not more than $2R \approx 20$ nm in diameter is realized via dissolution of coarse-dispersed metastable precipitates (Fig. 3*b*, *c*; II: $b \rightarrow c$), which are spaced by about $\Delta h \approx 10$ μm [4, 6, 7, 11–13]. Given this mechanism is actuated, stable TiC- and ZrC-based particles would form, for which the stoichiometric coefficients are equal to unity $\alpha = 1$, $\beta = 1$.

An application of intermediate anneals in the temperature interval 600– 700°C ((0.4–0.44) T_{melt}) during TMT II results in a lower diffusion activity of the phase-forming elements compared to that of interstitial impurities, which, according to relation (2), favors an increase in the kinetic parameter. Unfortunately, it does not seem possible to estimate this parameter due to the absence of the data on interstitial impurity diffusion at low temperatures. Note however that according to the present-day concepts, this parameter can be increased (by a few orders of magnitude) in the structural states with a high (more than 10^{10} cm^{-2}) dislocation density due to increased solubility and higher diffusion coefficients of the interstitial impurities in high defect states.

To sum up, a change in the TMT-modes (strain degree, intermediate annealing temperature), determining the kinetic parameter (K), offers a control over transformation of the structural-phase states and the level of strength properties.

SUMMARY

1. The data on the influence of the modes of thermomechanical treatment on the mechanical properties of vanadium alloys of different systems have been generalized. It has been found out that the use of thermomechanical treatment in the TMT II mode offers a considerable improvement of the short-term strength at an acceptable level of plasticity both at room temperature and elevated test temperatures.

2. An analysis of the conditions of thermomechanical treatment has demonstrated that a decrease in the intermediate annealing temperatures favors an increase of the kinetic parameter K and results in a change of the mechanism of metastable precipitate transformation. The phase transformations occur via the mechanism of dissolution

of metastable vanadium carbides, followed by precipitation of the stable phase from the solid solution, rather than by an ‘on site’ transformation.

The investigation has been performed using the equipment of the Tomsk Materials Center for Shared Use of Scientific Equipment at NR TSU.

This study has been carried out within the framework of the. Program of fundamental research of the state academies of sciences for 2013–2020, research line III.23.

REFERENCES

1. J. M. Chen, V. M. Chernov, R. J. Kurtz, and T. Muroga, J. Nucl. Mater., **417**, 289–294 (2011).
2. T. Muroga, J. M. Chen, V. M. Chernov, *et al*., J. Nucl. Mater., **455**, 263–268 (2014).
3. V. V. Shyrokov, Ch. B. Vasyliv, and O. V. Shyrokov, J. Nucl. Mater., **394**, 114–122 (2009).
4. A. N. Tyumentsev, A. D. Korotaev, Yu. P. Pinzhin, *et al*., VANT, Ser.: Materialoved. Nov. Mater., **2**, 111–122 (2004).
5. N. J. Heo, T. Nagasaka, and T. Muroga, J. Nucl. Mater., **325**, 53–60 (2004).
6. A. N. Tyumentsev, A. D.Korotaev, Yu. P. Pinzhin, *et al*., J. Nucl. Mater., **329**–**333**, 429–433 (2004).
7. I. A. Ditenberg, A. N. Tyumentsev, V. M. Chernov, and M. M. Potapenko, VANT, Ser.: Termoyad. Sint., **34,** No. 2, 28–35 (2011).
8. H. Y. Fu, J. M. Chen, P. F. Zhenga, *et al*., J. Nucl. Mater., **442**, S336–S340 (2013).
9. P. F. Zheng, T. Nagasaka, T. Muroga, *et al*., Fusion Eng. Des., **86**,. 2561–2564 (2011).
10. J. M. Chen, T. Nagasaka, T. Muroga, *et al*., J. Nucl. Mater., **374**, 298–303 (2008).
11. I. A. Ditenberg, A. N. Tyumentsev, K. V. Grinyaev, *et al*., Inorg. Mater. Appl. Res., **4**, No. 5, 438–443 (2013).
12. A. N. Tyumentsev, I. A. Ditenberg, K. V. Grinyaev, *et al*., VANT, Ser.: Termoyad. Sint., **37**, No. 1, 18–26 (2014).
13. I. A. Ditenberg, I. V. Smirnov, A. S. Tsverova, *et al*., Russ. Phys. J., **61**, No. 5, 936–941 (2018).
14. J. W. Martin, Micromechanisms in Particle-Hardened Alloys. Solid State Science Series, Cambridge University Press (1980).
15. J. P. Hirth and J. Lothe, Theory of Dislocations, Mc Graw-Hill, New York (1968).
16. J. Fridel, Dislocations, Pergamon Press, Oxford, New York, Paris (1964).
17. A. D. Korotaev, A. N. Tyumentsev, and V. F. Sukhovarov, Dispersion Hardening of Refractory Alloys [in Russian], Nauka, Novosibirsk (1989).
18. M. E. Smagorinskii, A. A. Bulyanda, and S. V. Kudryashov, Reference Book on Thermomechanical and Thermocyclic Treatment of Metals (Ed. M. E. Smagorinskii) [in Russian], Politekhnika, SPtb (1992).
19. B. A. Gnesin, A. P. Zuev, M. I. Karpov, *et al*., Fiz. Met. Metalloved., **60**, Iss. 5, 914–924 (1985).
20. I. I. Kornilov and V. V. Glazova, Interaction of Refractory Transition Metals with Oxygen [in Russian], Nauka, Moscow (1967).
21. B. S. Bokstein, Diffusion in Metals [in Russian], Metallurgiya, Moscow (1978).